AIP | Journal of Applied Physics

The comprehensive phase evolution for Bi2Te3 topological compound as function of pressure

S. J. Zhang, J. L. Zhang, X. H. Yu, J. Zhu, P. P. Kong et al.

Citation: J. Appl. Phys. **111**, 112630 (2012); doi: 10.1063/1.4726258
View online: http://dx.doi.org/10.1063/1.4726258
View Table of Contents: http://jap.aip.org/resource/1/JAPIAU/v111/i11
Published by the American Institute of Physics.

The comprehensive phase evolution for Bi_2Te_3 topological compound as function of pressure

S. J. Zhang,[1] J. L. Zhang,[1,2] X. H. Yu,[1,3] J. Zhu,[1] P. P. Kong,[1] S. M. Feng,[1] Q. Q. Liu,[1] L. X. Yang,[1] X. C. Wang,[1] L. Z. Cao,[2] W. G. Yang,[4] L. Wang,[4] H. K. Mao,[4] Y. S. Zhao,[5] H. Z. Liu,[3] X. Dai,[1] Z. Fang,[1] S. C. Zhang,[6] and C. Q. Jin[1,a)]

[1]*Institute of Physics, Chinese Academy of Sciences, Beijing 100190, China*
[2]*Department of Physics, University of Science and Technology of China, Hefei 230026, China*
[3]*Natural Science Research Center, Harbin Institute of Technology, Harbin 150080, China*
[4]*HPSynC, Geophysical Laboratory, Carnegie Institute of Washington, Argonne, Illinois 60439, USA and HPCAT, Geophysical Laboratory, Carnegie Institute of Washington, Argonne, Illinois 60439, USA*
[5]*LANSCE, Los Alamos National Laboratory, Los Alamos, New Mexico 87545, USA and HiPSEC, Department of Physics and Astronomy, University of Nevada, Las Vegas, Nevada 89154, USA*
[6]*Department of Physics, Stanford University, Stanford, California 94305-4045, USA*

(Received 11 May 2011; accepted 13 November 2011; published online 15 June 2012)

The recently discovered three-dimensional topological insulator Bi_2Te_3 is studied as function of pressure in terms of crystal structures, resistance, and Hall coefficient. The superconductivity is found in phase I (ambient phase) Bi_2Te_3 with $T_c \sim 3$ K, which is related to the topological features. The evolution of crystal structure with pressure is investigated by high pressure synchrotron radiation experiments that reveal structural transitions occurring at about 8 GPa, 13 GPa, and 16 GPa, respectively. Furthermore, the high pressure phases of Bi_2Te_3 are also superconducting but with much higher $T_c \sim 8$ K. The superconducting transitions are compared with those for Bi, Te elements. A global phase diagram of Bi_2Te_3 as function of pressure up to 30 GPa is obtained. © *2012 American Institute of Physics*. [http://dx.doi.org/10.1063/1.4726258]

INTRODUCTION

Topological insulator (TI) was theoretically predicated[1,2] and experimentally demonstrated[3–5] in recent years. Different from conventional insulators, TI has gapless and spin-split surface/edge states induced by bulk topological invariant property, which are protected by topological invariant such as the time-reversal symmetry as demonstrated in the two dimensional[3] or three dimensional TI system.[4–7] The unique property of these new types of quantum matter states attracts intensive attentions of worldwide research groups. Topological superconductor (TSC) that can support Majorana Fermions at its interface is much more fascinating[8–10] as its potential applications in topological quantum computation.[10] Considering the unique band structure in bulk states and surface/edge states of TI, searching for superconductivity in TI will be a ready way to approach topological superconductors since the surface can easily keep gapless topological nature. Recently, a new group of three dimensional topological insulators of Bi_2Se_3, Bi_2Te_3, etc., are discovered.[6] Superconductivity has been observed via copper doping in Bi_2Se_3 topological insulator,[11] i.e., using a chemical way to introduce carriers that result to superconductivity. More recently, we proposed an alternative way approaching topological superconductor via physical tool: using pressure to tune the electronic structure of Bi_2Te_3 TI.[12] It is well known that pressure is much effective in tuning superconductivity by changing electronic structure through directly modifying crystal parameters. Since pressure tuning is almost free of introducing impurities or defects comparing with chemical substitution, it will be more intrinsic to mechanism studies. Several groups have reported effects of pressure on Bi_2Te_3.[13–16] Previously superconductivity was observed above 9 GPa,[14] but the structure of Bi_2Te_3 changed to a new phase at these pressures. So it has no relation to the phase I (ambient pressure phase) of Bi_2Te_3 that was identified to be topological nontrivial.[6] We found that the superconductivity of Bi_2Te_3 is closely related to the carrier density at ambient pressure. In order to facilitate pressure induced superconductivity at lower pressure, i.e., within the ambient topological non trivial phase, it is necessary to slightly modify the carrier density of the parent compound to be around 10^{18}/cm^3. Based on successful growth of Bi_2Te_3 single crystals with the suitable carrier density, we indeed successfully observed superconductivity in the ambient topological non trivial phase of Bi_2Te_3 single crystals induced via pressure. The crystals remain well defined Dirac cone at its surface state for the superconductor indicating its topological nature.[12] Moreover, the aforementioned Bi_2Te_3 single crystals also show superconductivity in the high pressure phases but with much higher T_c than previously reported.[14] This enhanced superconductivity for high pressure phases is also related to the right carrier density. Here, we provide detailed investigations of pressure induced superconductivity in Bi_2Te_3 single crystals in combining with crystal structure studies using synchrotron diffractions. We discuss the evolution of electric conductivity, Hall coefficient as well as crystal structures in three distinctive pressure ranges: (I) within 8 GPa, wherein it keeps ambient structure with topological nontrivial; (II) in the intermediate high pressure region between 8 and 16 GPa; (III) in the higher pressure region above 16 GPa. To judge that superconducting transitions are not from compositional elements,

a)Author to whom correspondence should be addressed. Electronic mail: JIN@iphy.ac.cn.

we also compared the results with pressure induced superconductivity in Bi or Te elements. Based on electrical conductivity and synchrotron diffraction measurements, we obtained a general phase diagram of Bi_2Te_3 single crystals as function of pressure up to 30 GPa.

EXPERIMENTAL METHODS

Bi_2Te_3 single crystal was grown using Bridgeman method. Stoichiometric amounts of high purity elements Bi (99.999%) and Te (99.999%) were mixed, ground, and pressed into pellets, then loaded into a quartz Bridgeman ampoule, which was evacuated and sealed. The ampoule was placed in a furnace and heated at 800 °C for 3 days, after which it was slowly cooled in a temperature gradient at rate 5 °C per hour to 300 °C, followed by furnace cooling. The product was cleaved easily along the basal plane. The powder of Bi_2Te_3 grinded from single crystal was identified by x-ray powder diffraction.

Resistance measurement at high pressure of Bi_2Te_3 single crystal was performed by four-probe methods in a diamond anvil cell (DAC) made of CuBe alloy. A gasket made of T301 stainless steel was covered with insulating layer in order to protect the electrode leads from the metallic gasket. The electrodes were slim Au wires with 18 μm in diameter. The gasket, preindented from the thickness of 250 μm to 60 μm, was drilled a hole where MgO insulating layer was pressed. The dimension of Bi_2Te_3 single crystals for resistance experiments was typically about 90 μm $\times$ 90 μm $\times$ 10 μm with soft hBN fine powders around as pressure transmitting medium. The pressure was measured by ruby fluorescence method. The diamond anvil cell was put inside a Mag Lab system to perform the experiments. The temperature was automatically program controlled by the Mag Lab system. A thermometer was mounted nearby the diamond in the diamond anvil cell to monitor the sample temperature accurately. The decrease of temperature was very slow to make sure the equilibrium of temperature. The Hall coefficient at high pressure was measured using Van der Pauw method. The details of experimental operation can be found in Ref. 12.

The x-ray diffraction experiments at high pressure at room temperature with synchrotron radiation were done at the HPCAT of Advanced Photon Source (APS) of Argonne National Lab (ANL) with a wavelength 0.368 Å using a symmetric Mao Bell diamond anvil cell at room temperature. The crystal structures were refined by GSAS package.[17]

RESULTS AND DISCUSSION

Bi_2Te_3 has a rhombohedral structure at ambient pressure with a space group R-3 m, as shown in Fig. 1. Along the c axis direction, the unit cell contains five atomic layers with a stacking sequence of Te(1)-Bi-Te(2)-Bi-Te(1), forming unique quintuple layer (QL). The QL is terminated by Te(1) atomic layer in both sides. The interaction between two adjacent QLs is of the van der Waals type, which is much weaker than that between two atomic layers within a QL, yielding a material with excellent basal plane cleavage and layered crystals. Its crystal parameters are a = 4.3852 Å and

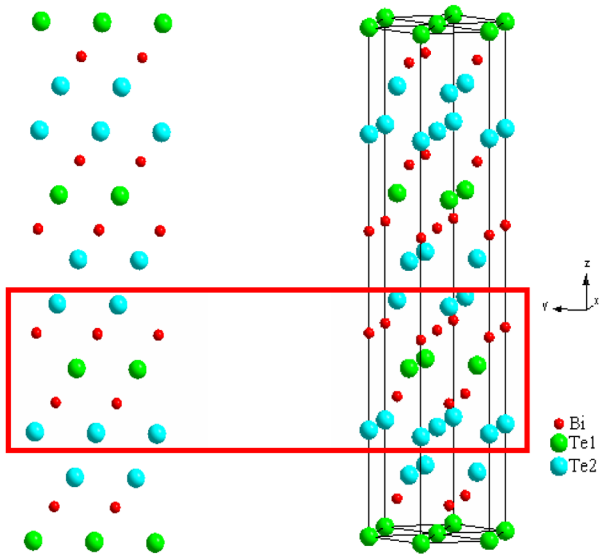

FIG. 1. The crystal structure of Bi_2Te_3 with space group R-3 m.

c = 30.483 Å, respectively, at ambient pressure and room temperature. The layered structure leads Bi_2Te_3 a good model to investigate the TI properties.[18] The Hall coefficient measurements indicate the p-type carrier nature of Bi_2Te_3 sample used in the experiments.[12] The carrier density calculated from the linear part at high magnetic field is approximately 3–6 $\times$ 10^{18}/cm^3, which is deduced from several measurements at ambient pressure. The Hall coefficients as function of pressure at 30 K deduced from the linear part at high magnetic field of high pressure Hall measurements are shown in Fig. 2. It is found that the carrier type is unchanged until 7 GPa although Hall coefficient is decreasing since the crystals become more metallic with pressure, i.e., the carrier density has been increasing with pressure. The calculated carrier density changes from 6 $\times$ 10^{18} at 3 GPa to 3 $\times$ 10^{22} at 6.8 GPa with sudden increase at about 5 GPa. The resistance measurements of p-type Bi_2Te_3 single crystals are performed under pressure. Fig. 3 shows its superconductivity induced by pressure at phase I (ambient phase), phase II (high pressure phase I, HP I), phase III (high pressure phase II, HP II), and phase IV (high pressure phase III, HP III), respectively

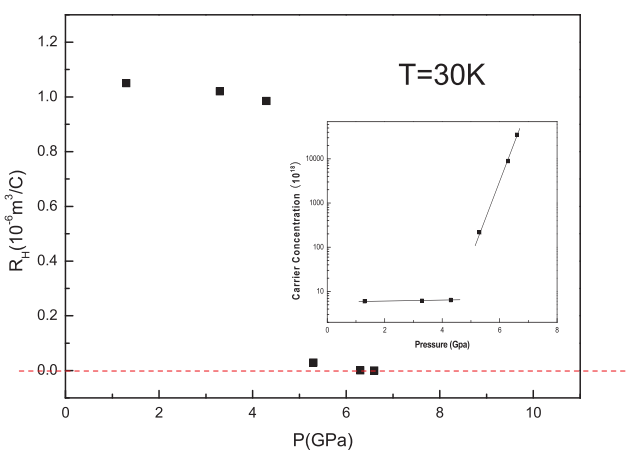

FIG. 2. The Hall coefficients as function of pressure at 30 K up to 6.8 GPa. The carrier type of p-type Bi_2Te_3 does not change until 6.8 GPa.

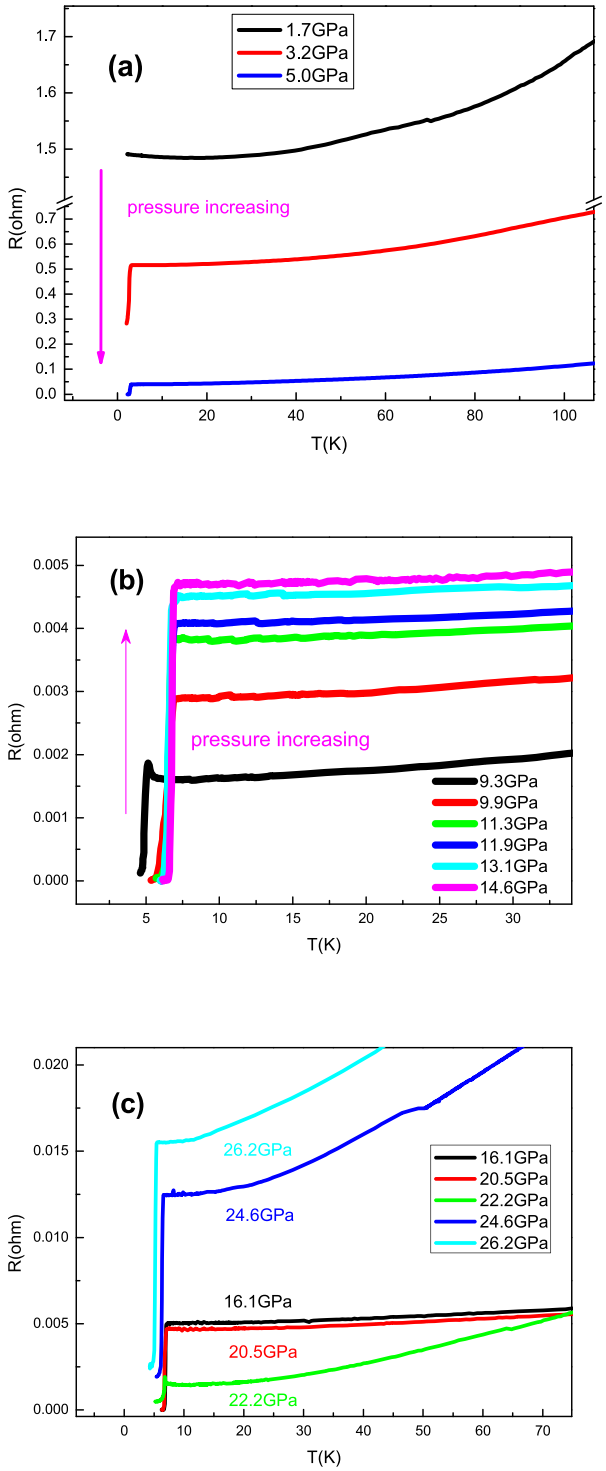

FIG. 3. The resistance of Bi_2Te_3 single crystal as function of temperature at various pressures showing superconductivity at phase I (a); HP I (II) (b); HP III (c).

(will discuss more detail for high pressure phase transition). The superconductivity occurs at about 3 GPa originally, as shown in Fig. 3(a) with the superconducting transition temperature (T_c) about 3 K. T_c increases slowly at the beginning while the resistance of normal state decreases with increasing pressure. Fig. 3(b) shows the superconducting transition from 9.3 to 15 GPa where a much higher $T_c \sim 8$ K was observed in the high pressure phases as we will discussed based on structure experiments. With increasing pressure, the transition temperature increases slowly, but its resistance of normal state starts to increase abnormally since the structural transition takes place. The superconducting transition temperature at pressures above 16 GPa decreases slowly with pressure, as shown in Fig. 3(c). Its resistance of normal state decreases first, and then increases rapidly at pressures above 22 GPa. At phase I, the upper critical field $H_{c2}(0)$ was extrapolated to be 1.8 Tesla for $H_{\|c}$ using the Werthdamer-Helfand-Hohenberg formula[20] of $H_{c2}(0) = -0.691[dH_{c2}(T)/dT]_{T=Tc} \times T_c$ as calculated in Ref. 12. The resistance curves as function of temperature with applied magnetic field H of high pressure phases are shown in Figs. 4(a) and 4(b), respectively, with insets showing the change of T_c with H. We get the upper critical field $H_{c2}(0) \sim 4.2$ Tesla at 9 GPa for HP I(II) and 2.1 Tesla at 30 GPa for HP III using the same method in Ref. 12, respectively.

The results of high pressure synchrotron radiation experiments indicate the evolution of crystal structure with pressure as shown in Fig. 5. All the reflections obtained at 2.2 GPa are well indexed by space group R-3 m, corresponding to the

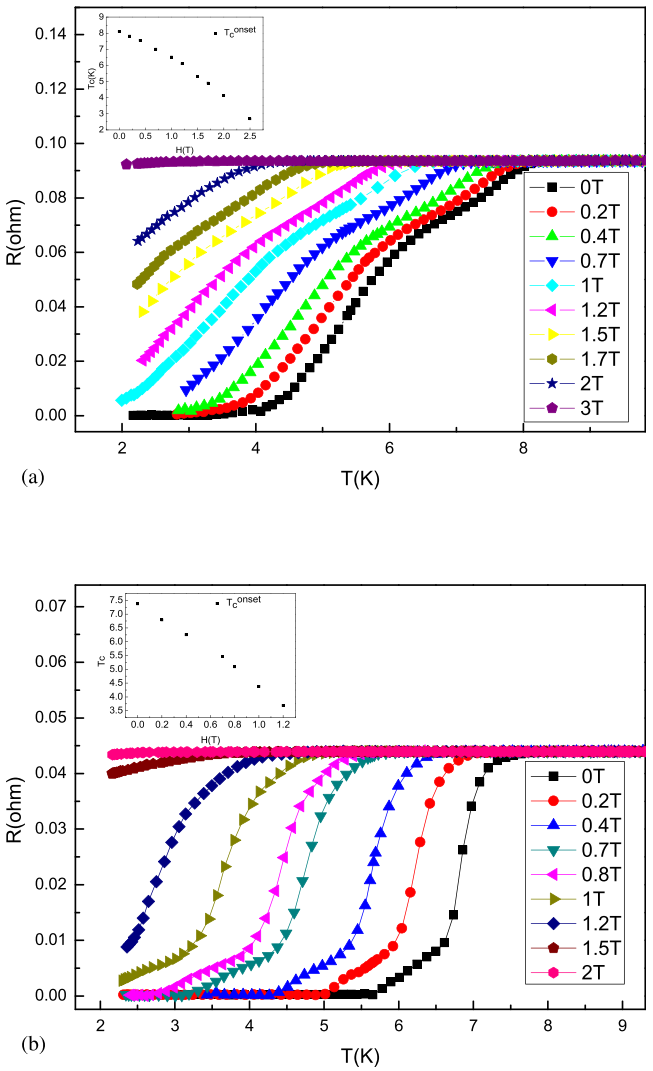

FIG. 4. The superconducting transition of Bi_2Te_3 with applied magnetic field H perpendicular to the ab-plane of single crystal at 9 GPa (a) and 30 GPa (b). Insets show the change of T_c with H, the upper critical fields $H_{c2}(0)$ are extrapolated to be 4.2 T and 2.1 T, respectively, using the Werthdamer-Helfand-Hohenberg formula.

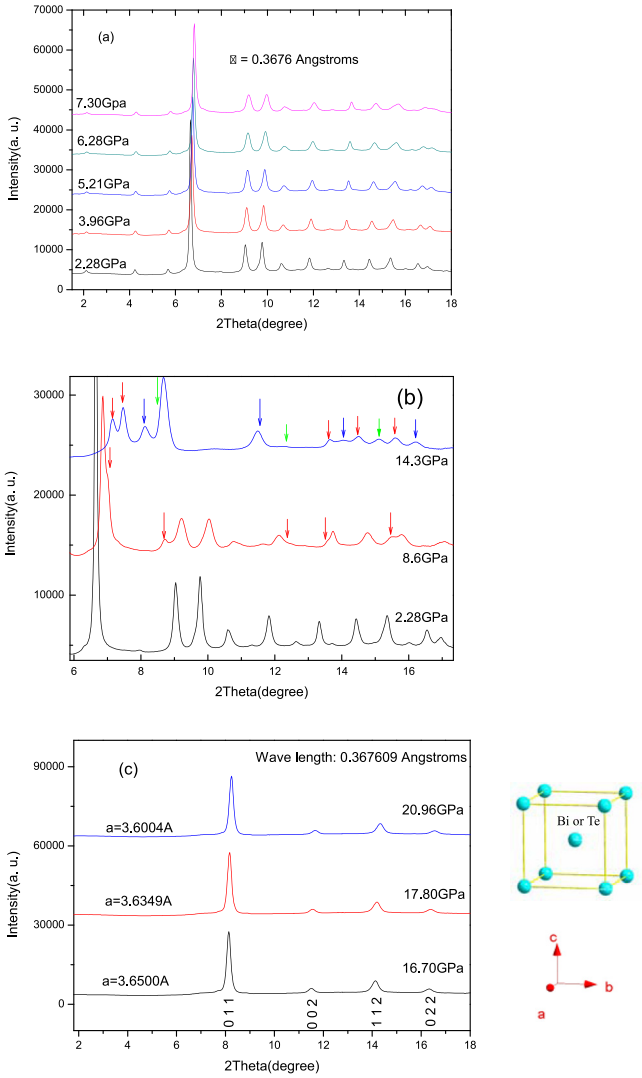

FIG. 5. (a) The evolution of x-ray diffraction reflections with pressure at phase I. No new reflection emerges lower than 8 GPa; (b) The red (8.6 GPa), green (14.3 GPa), and blue (14.3 GPa) arrows indicate new reflections of HP I, HP II, and HP III, respectively, induced by pressure; (c) The evolution of x-ray diffraction reflections with pressure at HP III, which has BCC structure with Im-3 m space group. A charge transfer from Bi to Te leads to the random distribution of Bi and Te atoms on the BCC sites.

phase I. Fig. 5(a) shows the evolution of reflections with pressure of phase I. No structural transition occurs at pressure lower than 8 GPa. Some new reflections which are denoted by arrows in Fig. 5(b) show the high pressure phases above 8 GPa for HP I and at 14.3 GPa for HP II and HP III, respectively. HP II was reported in Ref. 16, which can only stabilize in a narrow pressure range and coexists with either HP I or HP III. In our experimental results, the reflections from HP I marked by red arrows are observed at pressures above 8 GPa; while some reflections marked by green and blue arrows that differ from the HP I reflections are observed at about 14 GPa, which are assigned to HP II and HP III, respectively. The simple reflection peaks of high pressure phase as shown in Fig. 5(c) above 16 GPa indicate its high symmetric crystal structure. Actually it can be assigned to a body centered cubic (BCC) crystal structure with lattice parameters a = 3.6500 Å at 16.8 GPa. We indexed the x ray diffraction patterns of the BCC structure for the diffraction patterns above 16 GPa. Within the BCC structure, Bi and Te atoms are disordered to share the BCC lattice sites. This may be obtained at high pressure when A and B ion radii are nearly equal caused by charge transfer from Bi to Te. This is in good agreement with the previous report.[16] More recently, possible phases for intermediated high pressure phases of HP I and HPII are suggested to be of monoclinic sevenfold C2/m structure and eightfold C2/c structure respectively.[19] Fig. 6 shows the structural phase diagram of Bi_2Te_3 as function of pressure up to 30 GPa with the possible space groups of high pressure phases.

The superconducting transition temperature as function of pressure up to 30 GPa for Bi_2Te_3 is obtained by high pressure resistance measurements. The transition temperatures of high pressure phases are about 8 K, comparable to that of Bi or Te elements.[21,22] To judge the origination of superconductivity, we observed for Bi_2Te_3 single crystal the pressure tuned superconductivity of Bi and Te elements are also investigated using high pressure resistance experiments. Fig. 7(a) shows the resistance as function of temperature at different pressures for element Bi, whose superconducting transition occurs at about 3.5 GPa. Fig. 7(b) shows the resistance as function of temperature at different pressures for element Te, whose superconducting transition occurs at much higher than 20 GPa. We compare the superconductivity of Bi_2Te_3 with Bi or Te elements in Fig. 7(c), indicating that the superconductivity of Bi_2Te_3 is from neither Bi nor Te. It means that the superconductivity of Bi_2Te_3 single crystal at ambient phase and high pressure phases are indeed intrinsic natures itself.

The first superconducting transition with $T_c \sim 3$ K can be topological at the surface state possible proximity effects. It is theoretically predicated that the proximity effects between an s wave bulk superconductivity and the surface of a strong TI can cause topological superconductivity at surface state with $p_x + ip_y$ symmetry.[8] The other more exiting possibility is that the superconductivity of the ambient phase is truly three dimensional in a similar way similar to the

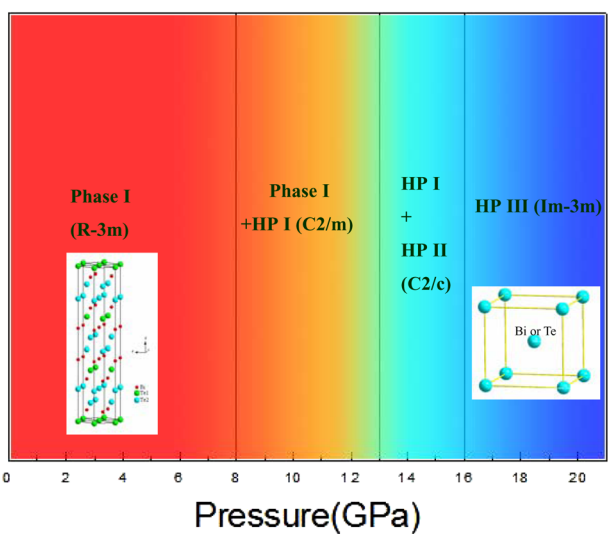

FIG. 6. The crystal structure phase diagram of Bi_2Te_3: the phase I from 0 to 8 GPa has a rhombohedral R-3 m structure; the HP I (8∼16 GPa), HP II (13∼16 GPa), and HP III (>16 GPa) have monoclinic sevenfold C2/m structure, eightfold C2/c structure, and BCC Im-3 m structure, respectively.

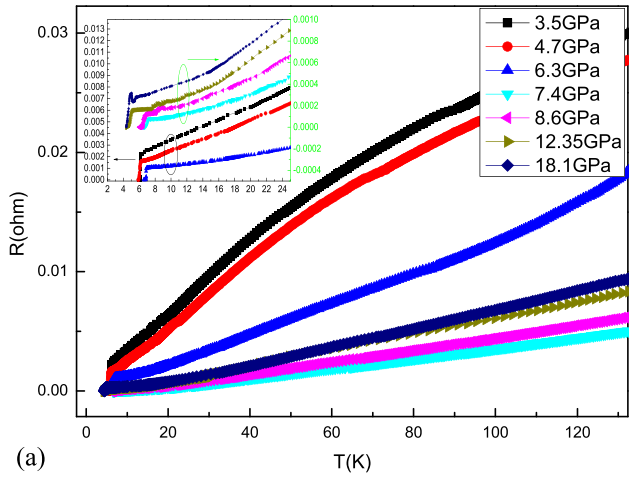

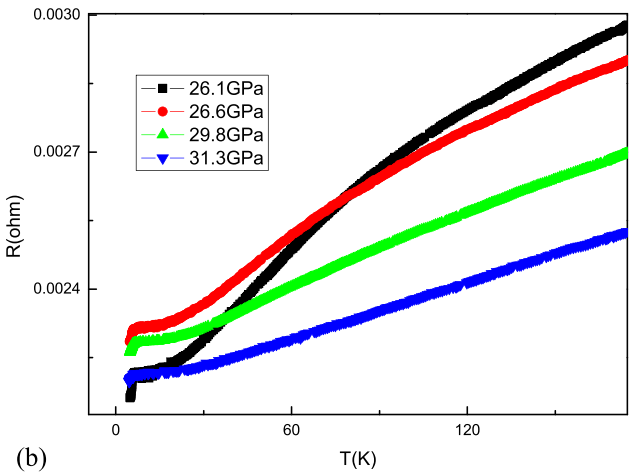

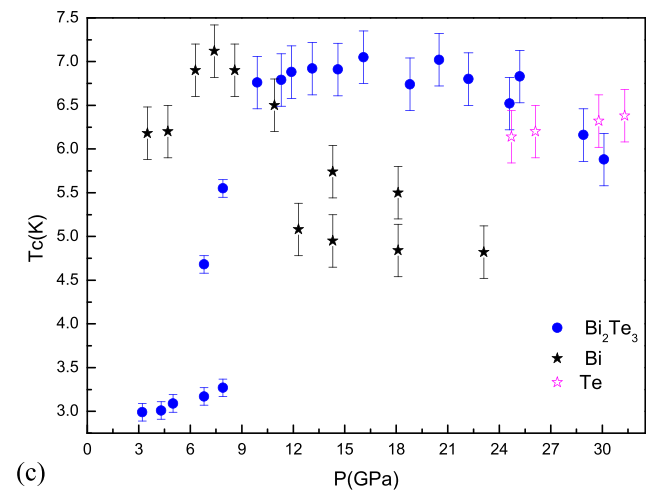

FIG. 7. (a) The resistance of Bi as function of temperature at various pressures showing superconductivity above 3.5 GPa; (b) the resistance of Te as function of temperature at various pressures showing superconductivity above 26 GPa; (c) the comparison of superconductivity of Bi_2Te_3, Bi, and Te with the error bars marked.

Balian and Werthamer state in He3 B phase.[12] Before the first structural transition from rhombohedral structure to monoclinic sevenfold C2/m structure, a parallel movement of $BiTe_6$ along the [110] direction probably starts to take place as a result of the distortion of crystal induced by pressure. The induced change of electrical structure may lead to the increase of transition temperature. Around the first structural transition at about 8 GPa, the resistance of normal state increases abnormally with pressure, consistent with the transition from phase I to HP I. Simultaneously, the superconducting transition temperature increases more slowly. The same phenomenon is found for HP II where T_c also slightly increases with pressure. But it is quite different that T_c becomes decreased above 16 GPa in HP III phase region.

Fig. 8 shows the superconductive phase diagram of p-type Bi_2Te_3 single crystal as function of pressure. The blue part is related to topological superconducting phase of phase I; the superconducting transition temperatures of high pressure phases are much higher than that of phase I. The samples show superconductivity in the whole pressure range for the high pressure phases up to 30 GPa.

In summary, a global phase diagram of Bi_2Te_3 as function of pressure is obtained in combination with electric conductivity as well as structure studies. First, we found superconductivity in ambient phase I of Bi_2Te_3 with pressure from 3 to 8 GPa, with topological nature as suggested by first principle calculations. The compound is superconducting for the high pressure phases at all range of pressure measurements up to 30 GPa but with much higher T_c around 8 K. The Hall measurements indicated the carries density increases with pressure but keeps p type at least up to 8 GPa. The Upper critical magnetic fields are calculated to be 1.8 T, 4.2 T, and 2.1 T for phase I, HP I (II), and HP III, respectively. The superconducting results of Bi_2Te_3 are compared with those for Bi or Te elements. Second, the high pressure crystal structure experiments with synchrotron diffraction indicate a series of phase transitions at ~8 GPa, in between 8 and 16 GPa, and above 16 GPa. A BCC high pressure phase is identified above 16 GPa that shows a Bi and Te soluble alloy of space group Im-3 m with lattice parameter a = 3.6500 Å. Based on the systematic studies, we established a comprehensive superconducting and structural phase diagram for Bi_2Te_3 topological compound.

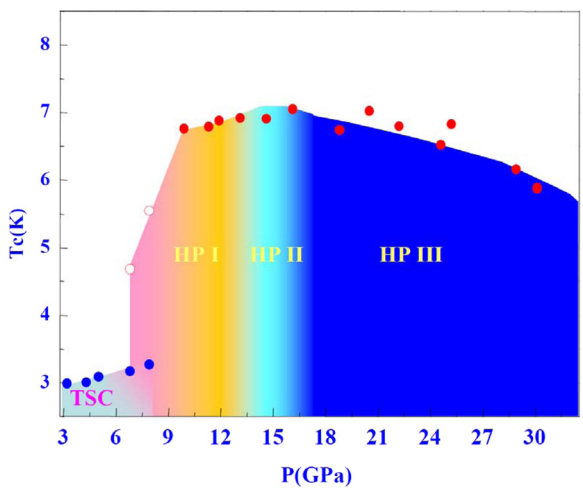

FIG. 8. The superconducting phase diagram of Bi_2Te_3 single crystal as function of pressure. The symbols represent experimental data; the color area belongs to the range of superconducting phases. The blue part (3-8 GPa) is related to the TSC range with phase I structure.

ACKNOWLEDGMENTS

We thank the supports from the NSF and MOST of China through the research projects and the International Science and Technology Cooperation Program of China. We are grateful to Dr. Guoyin Shen and the beam line scientist at BMD of HPCAT for their helps during the synchrotron experiments at Advance Photon Source. HPSynC is supported as part of EFree, an Energy Frontier Research Center funded by DOE-BES under Award No. DE-SC0001057.

[1]B. A. Bernevig, T. L. Hughes, and S.-C. Zhang, Science **314**, 1757 (2006).
[2]L. Fu and C. L. Kane, Phys. Rev. B **76**, 045302 (2007).
[3]M. König, S. Wiedmann, C. Brüne, A. Roth, H. Buhmann, L. W. Molenkamp, X.-L. Qi, and S.-C. Zhang, Science **318**, 766 (2007).
[4]D. Hsieh, D. Qian, L. Wray, Y. Xia, Y. S. Hor, R. J. Cava, and M. Z. Hasan, Nature **452**, 970 (2008).
[5]Y.-L. Chen, J. G. Analytis, J.-H. Chu, Z.-K. Liu, S.-K. Mo, X.-L. Qi, H.-J. Zhang, D.-H. Lu, X. Dai, Z. Fang, S.-C. Zhang, I. R. Fisher, Z. Hussian, and Z.-X. Shen, Science **325**, 178 (2009).
[6]H. J. Zhang, C. X. Liu, X. L. Qi, X. Dai, Z. Fang, and S. C. Zhang, Nat. Phys. **5**, 438 (2009).
[7]Y. Xia, D. Qian, D. Hsieh, L. Wray, A. Pal, H. Lin, A. Bansil, D. Grauer, Y. S. Hor, R. J. Cava, and M. Z. Hasan, Nat. Phys. **5**, 398 (2009).
[8]L. Fu and C. L. Kane, Phys. Rev. Lett. **100**, 096407 (2008).
[9]X. L. Qi, T. L. Hughes, S. Raghu, and S. C. Zhang, Phys. Rev. Lett. **102**, 187001 (2009).
[10]A. Kitaev, Ann. Phys. **321**, 2 (2006).
[11]Y. S. Hor, A. J. Williams, J. G. Checkelsky, P. Roushan, J. Seo, Q. Xu, H. W. Zandbergen, A. Yazdani, N. P. Ong, and R. J. Cava, Phys. Rev. Lett. **104**, 057001 (2010).
[12]J. L. Zhang, S. J. Zhang, H. M. Weng, W. Zhang, L. X. Yang, Q. Q. Liu, S. M. Feng, X. C. Wang, R. C. Yu, L. Z. Cao, L. Wang, W. G. Yang, H. Z. Liu, W. Y. Zhao, S. C. Zhang, X. Dai, Z. Fang, and C. Q. Jin, Proc. Natl Acad. Sci. U.S.A. **108**, 24 (2011).
[13]M. K. Jacobsen, R. S. Kumar, A. L. Cornelius, S. V. Sinogeiken, and M. F. Nicol, AIP Conf. Proc. **955**, 171 (2007).
[14]M. Einaga, Y. Tanabe, A. Nakayama, A. Ohmura, F. Ishikawa, and Y. Yamada, J. Phys.: Conf. Ser. **215**, 012036 (2010).
[15]A. Nakayama, M. Einaga, Y. Tanabe, S. Nakano, F. Ishikawa, and Y. Yamada, High Press. Res. **29**, 245 (2009).
[16]M. Einaga, A. Ohmura, A. Nakayama, F. Ishikawa, Y. Yamada, and S. Nakano, Phys. Rev. B **83**, 092102 (2011).
[17]B. H. Toby, J. Appl. Cryst. **34**, 210 (2001)
[18]X.-L. Qi and S.-C. Zhang, Phys. Today **63**(1), 33 (2010).
[19]L. Zhu, H. Wang, Y. C. Wang, J. Lv, Y. M. Ma, Q. L. Cui, Y. M. Ma, and G. T. Zou, Phys. Rev. Lett. **106**, 145501 (2011).
[20]N. R. Werthamer, E. Helfand, and P. C. Hohenberg, Phys. Rev. **147**, 295 (1966).
[21]M. A. Il'ina and E. S. Itskevich, ZhETF Pis. Red. **11**, 328 (1970).
[22]Y. Akahama, M. Kobayashi, and H. Kawamura, Solid State Commun. **84**, 803 (1992).